# Supplementary Information

# Inhibiting Selenium Loss in Sodium-Selenium Batteries via a Lewis Acid-Base Dual-Site Host

Rui Wang[a], Guoqiang Yuan[a], Lin Ding[a], Yuan Gao[ac], Yan Dong[b], Wenting Li*[a] and Huan Pang*[a]

*a. School of Chemistry and Materials, Yangzhou University, Yangzhou 225002, PR China.*

*b. Suzhou Institute of Nano-Tech and Nano-Bionics, Chinese Academy of Sciences, Suzhou 215123, P.R. China.*

*c. Interdisciplinary Research Center for Advanced Energy, Yangzhou University, Yangzhou, Jiangsu 225127, P. R. China.*

*Corresponding authors:

E-mail: wtlichem@yzu.edu.cn (W.T. Li); huanpangchem@hotmail.com (H. Pang).

## Experimental Procedures

### 1.1 Preparation of NHMCS

Ammonia (10 mL), tetraethyl orthosilicate (12 mL), resorcinol (1.6 g), and formaldehyde (2.4 mL) were added to the mixture of ethanol (1600 mL) and deionized water (20 mL), and magnetic stirring was performed for 24 h. After centrifugation, $SiO_2$@RF (resorcinol-formaldehyde) composite was obtained (6000 rpm, 5 min). After cooling to room temperature, it was calcined at 700 ℃ for 6 h in a tubular furnace. Then the silica was removed by NaOH solution at 80 ℃ to obtain Nitrogen-doped hollow mesoporous carbon nanospheres (NHMCS).

### 1.2 Preparation of NB@HMCS

Typically, NHMCS and boric acid were mixed at a mass ratio of 1:3 and thoroughly ground for 30 min. The obtained mixture was then annealed at 800 °C for 2 h under an Ar atmosphere with a heating rate of 5 °C $min^{-1}$. After naturally cooling to room temperature, the resulting product was collected and denoted as NB@HMCS. During the annealing process, boric acid served as the boron source, resulting in the successful construction of Lewis acid–base dual active sites within the carbon framework.

### 1.3 Preparation of Se/C cathode

200 mg of NB@HMCS and 600 mg of selenium were mixed and heated in a tubular furnace at 2 ℃ $min^{-1}$ at 260 ℃ for 12 h in $N_2$ atmosphere. The final product

was collected and labeled Se/NB@HMCS. Se/NB@HMCS composite, carbon black, and PVDF were mixed in NMP solvent at a mass ratio of 8:1:1 to prepare the paste. The stirred slurry was coated on the aluminum foil collector and vacuum dried at 120 ℃ for 10 h. The mass loading for each sample was 1.6-2.0 mg $cm^{-2}$. The CR2032 coin battery, used a glassy fiber as the diaphragm, a sodium metal sheet as the reference electrode, and 1 M $NaClO_4$ in EC/PC (1:1) as the electrolyte, was assembled in a glovebox filled with high purity argon (Vacuum Co., Ltd.).

All the chemicals used above are analytical pure products produced by Aladdin.

**1.4 Characterization**

FESEM images were performed on Zeiss Supra55. TEM images were taken from the TECNAI-12 instrument. HRTEM images were conducted on G2 F30 STWIN (USA). XRD analysis was performed by Cu-Ka D8 ultrafast powder diffraction (Bruker). XPS data were obtained from the Thermo Escalab 250 system. The adsorption and desorption isotherms of $N_2$ were recorded by ASAP 2020 and HD88 at 180 ℃. The specific surface area of the samples was determined by the BET method and the pore size distribution was calculated by the BJH method. The bottle used to soak the electrode is screw mouth glass sample bottle (NINGKEE), the size is 18mm*40mm. Thermogravimetric analysis (TGA) was performed on a NETZSCH STA 449 F3 thermal analyzer from room temperature to 800 °C at a heating rate of 10 °C $min^{-1}$ under a nitrogen atmosphere to determine the selenium content in the composites.

### 1.5 Electrochemical characterization

The batteries were assembled in a glove box filled with high-purity argon gas. Charge and discharge tests were carried out on the battery test system (CT-3008W, Xinwei, CHN), and the rate performance and cycle stability performance were tested. The calculation method is to obtain the specific capacity by using the ratio of discharge capacity to electrode mass, where the electrode mass is the total mass. Cyclic voltammetry (CV) and electrochemical impedance spectroscopy (EIS) experiments were conducted with an electrochemistry workstation (CHI660E, Chenghua, CHN). CV measurements for Na-Se batteries were made at a scanning rate of 0.1 mV $s^{-1}$ over a range of 0.5-3.0 V (vs $Na/Na^{+}$). EIS test frequencies range from 100 kHz to 0.01 Hz.

### 1.6 DFT calculation

First-principles calculations were performed using the Vienna Ab-initio Simulation Package (VASP). The Perdew-Burke-Ernzerhof (PBE) generalized gradient approximation (GGA) was utilized for the exchange-correlation energy calculation. To account for the van der Waals (vdW) interactions in the systems, the DFT-D3 method developed by Grimme was applied. The Projector Agmented-Wave (PAW) method with a plane-wave basis set with an energy cut-off of 450 eV was used for total energy calculations. The force and energy convergence criterions were set to be 0.02 eV $Å^{-1}$ and $10^{-5}$ eV, respectively. To eliminate interactions between adjacent unit cells, a vacuum separation >15 Å was employed. The first Brillouin Zone was sampled using a k-point mesh of 4 × 4 × 1. The binding energy ($E_b$) of $Na_2Se_x$ was defined as: Eb =

$E_{slab+Na2Sex}$ - $E_{slab}$ - $E_{Na2Sex}$, where $E_{slab}$ is the energy of NHMCS and NB@HMCS, respectively. $E_{Na2Sex}$ is the energy of $Na_2Se_x$, and $E_{slab+Na2Sex}$ is the total energy of the $Na_2Se_x$ adsorbed on the corresponding surface. The climbing-image nudged elastic band (CI-NEB) method was employed to calculate the barriers for $Na_2Se$ diffusion on NHMCS and NB@HMCS, respectively.

The relative free energy of the discharging process from $Se_8$ to $Na_2Se$ on the substrate was calculated following the reaction sequence of

$$Se_8 + Na \overset{(1)}{\rightarrow} Na_2Se_8 \overset{(2)}{\rightarrow} Na_2Se_6 \overset{(3)}{\rightarrow} Na_2Se_4 \overset{(4)}{\rightarrow} Na_2Se_2 \overset{(5)}{\rightarrow} Na_2Se_1$$

The corresponding reaction energies for the five steps are calculated from the equations (1–5), respectively:

$$E_{Na_2Se_8 + sbustrate} - E_{Se_8 + substrate} - 2E_{Na} \quad \text{* MERGEFORMAT (1)}$$

$$E_{Na_2Se_6 + substrate} + \frac{1}{4}E_{Se_8} - E_{Na_2Se_4 + substrate} \quad \text{* MERGEFORMAT (2)}$$

$$E_{Na_2Se_4 + substrate} + \frac{1}{4}E_{Se_8} - E_{Na_2Se_6 + substrate} \quad \text{* MERGEFORMAT (3)}$$

$$E_{Na_2Se_2 + substrate} + \frac{1}{4}E_{Se_8} - E_{Na_2Se_6 + substrate} \quad \text{* MERGEFORMAT (4)}$$

$$E_{Na_2Se_1 + substrate} + \frac{1}{8}E_{Se_8} - E_{Na_2Se_2 + substrate} \quad \text{* MERGEFORMAT (5)}$$

where $E_{Na}$ is the energy of sodium atom and $E_{Se8}$ is the gas-phase energy of $Se_8$.

**1.7 Finite element method (FEM)**

Finite element simulations were carried out using COMSOL Multiphysics 6.2 to investigate sodium-ion transport behavior on different host surfaces. A simplified 4 × 4 host-material array was constructed according to the experimentally observed morphology to compare ion transport characteristics between NHMCS and NB@HMCS hosts.

The diffusion of ion concentrations follows Fick's first law, and the reaction at the electrode surface follows the Butler–Volmer equation. The $Na^+$ transfers by the concentration diffusion in the model follow Fick's law as shown in equations:

$$N_i = J_i = -D_i \nabla C_i$$

$$\frac{\partial C_i}{\partial t} + \nabla J_i = R_{i,\,tot}$$

Where $J_i$ is the ion flux, $D_i$ is the diffusion coefficient of $Na^+$, $C_i$ is the ion concentration of $Na^+$, $\nabla C_i$ is the concentration gradient. The relation between the diffusion coefficient and electric mobility follows the Nernst-Einstein relation as shown in the equation:

$$N_i = -D_i \nabla c_i - z_i \mu_{m,\,i} F c_i \nabla \phi_l + \mu c_i = J_i + \mu C_i$$

Where $z_i$ is the transfer number, $\mu_{m,i}$ is the electric mobility coefficient, F is the Faraday constant (96485 C $mol^{-1}$), $\phi$ is the electrolyte potential.

The reaction at the electrode surface follows the Butler-Volmer equation:

$$i_{loc} = i_0 \left( \exp\left( \frac{\alpha_a F \eta}{RT} \right) - \exp\left( \frac{-\alpha_a F \eta}{RT} \right) \right)$$

Where $i_{loc}$ is the local current density at the electrode/electrolyte interface, $i_0$ is the exchange current density, $\alpha$ is the charge transfer coefficient, and $\eta$ is the activation

overpotential.

The initial $Na^+$ concentration was normalized to 1.0 a.u. for comparative simulation.

The diffusion coefficient of sodium ions was set to $1\times10^{-10}$ $m^2$ $s^{-1}$ according to previously reported values.

An electric field of 100 mV $m^{-1}$ was applied along the vertical direction.

The upper boundary was defined as the sodium-ion inlet, while the lower boundary was defined as the outlet. The lateral boundaries were set as no-flux boundaries.

**Supplementary figures**

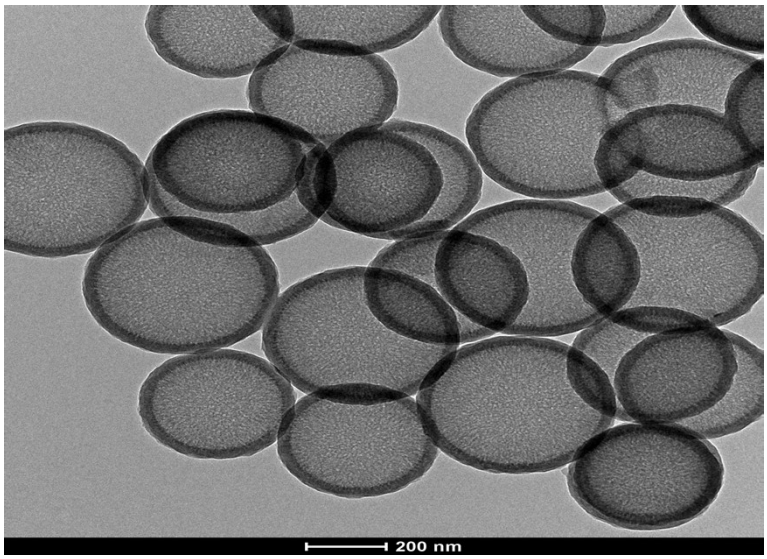


Fig. S1 TEM image of NHMCS host.

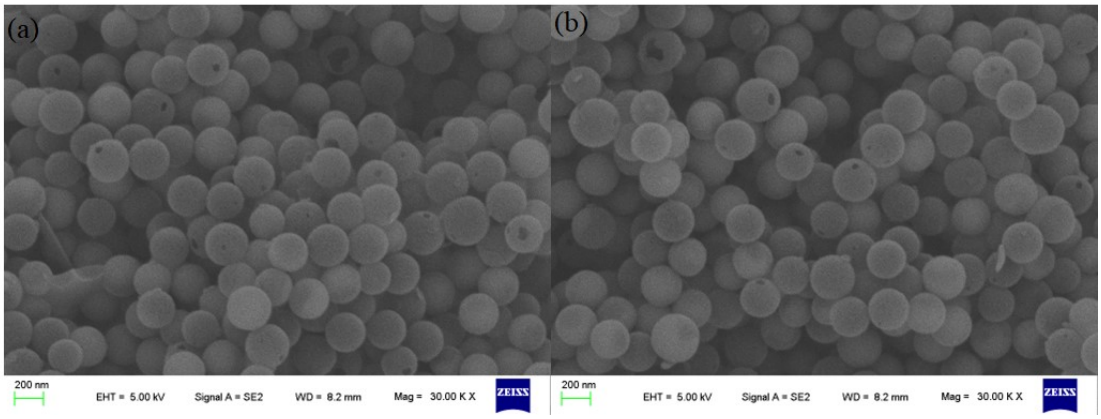


Fig. S2 SEM images of (a) Se/NHMCS and (b) Se/NB@HMCS.

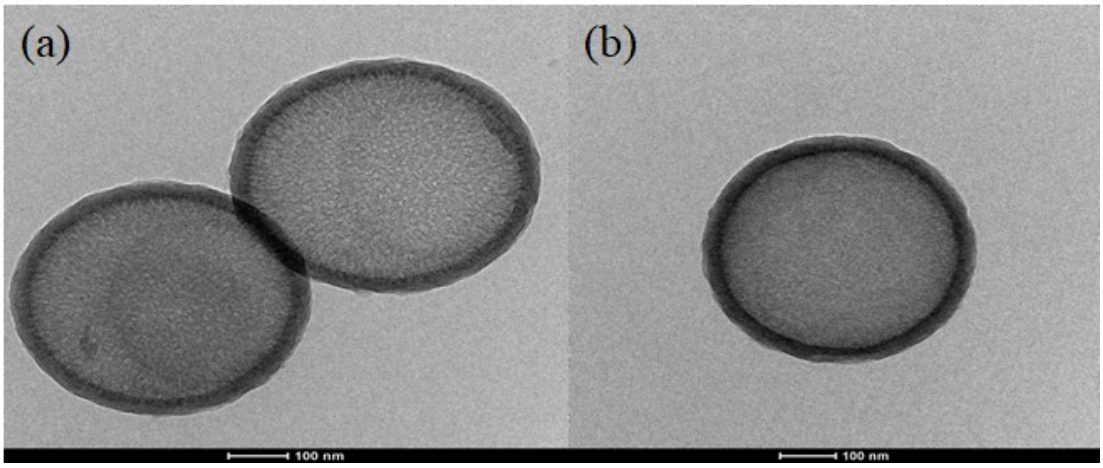


Fig.S3 TEM images of (a) Se/NHMCS and (b) Se/NB@HMCS.

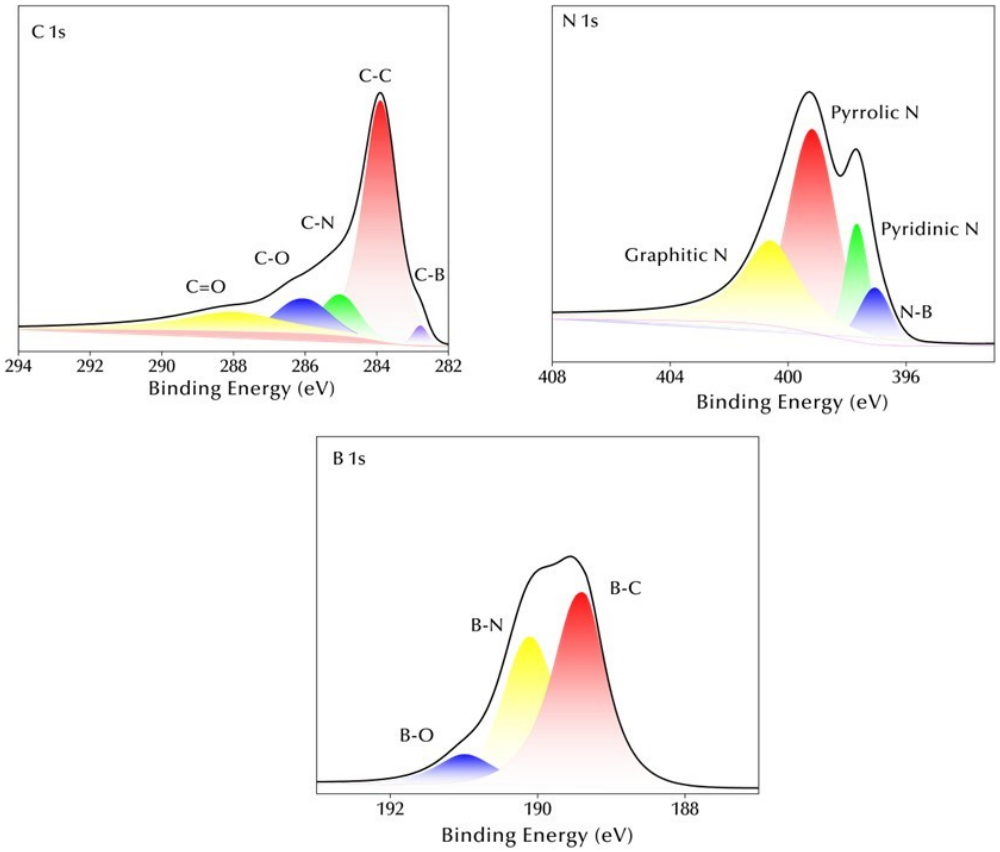


Fig. S4 XPS high-resolution spectra of C 1s, N 1s and B 1s in NB@HMCS host.

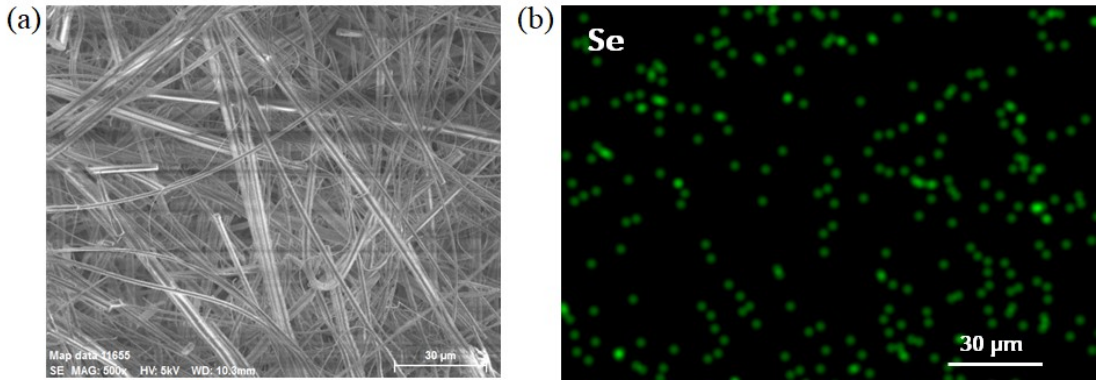


Fig. S5 (a) SEM image of GF separator in Na||Se/NB@HMCS batteries after 100 cycles at 0.2C, (b) Corresponding selenium element mapping distribution.

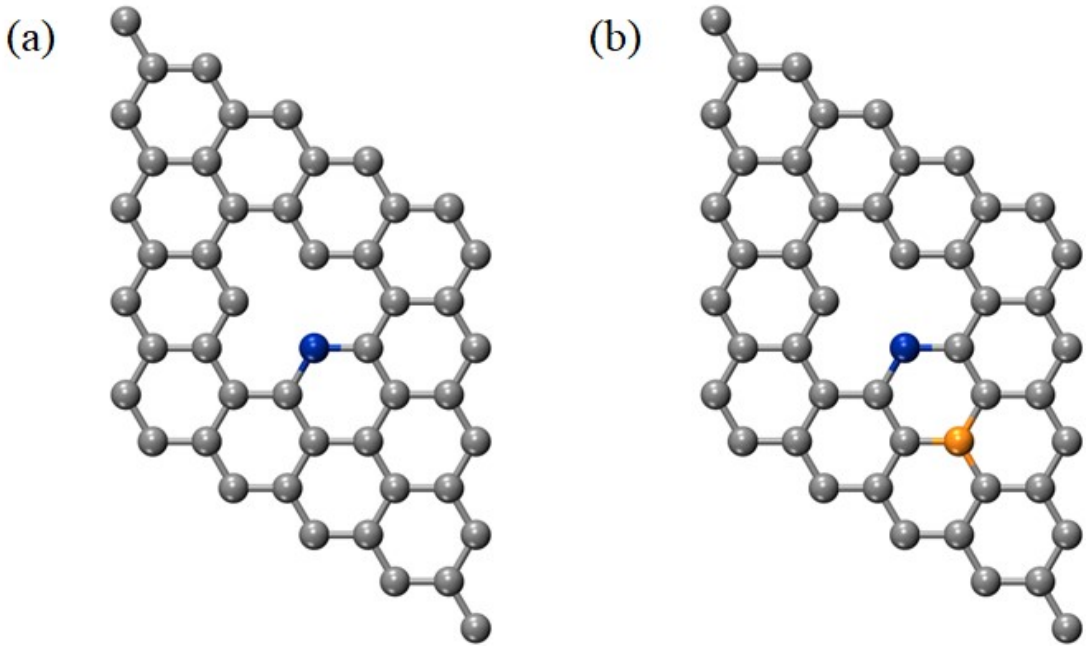


Fig. S6 Geometric optimization model of (a) NHMCS and (b) NB@HMCS hosts.

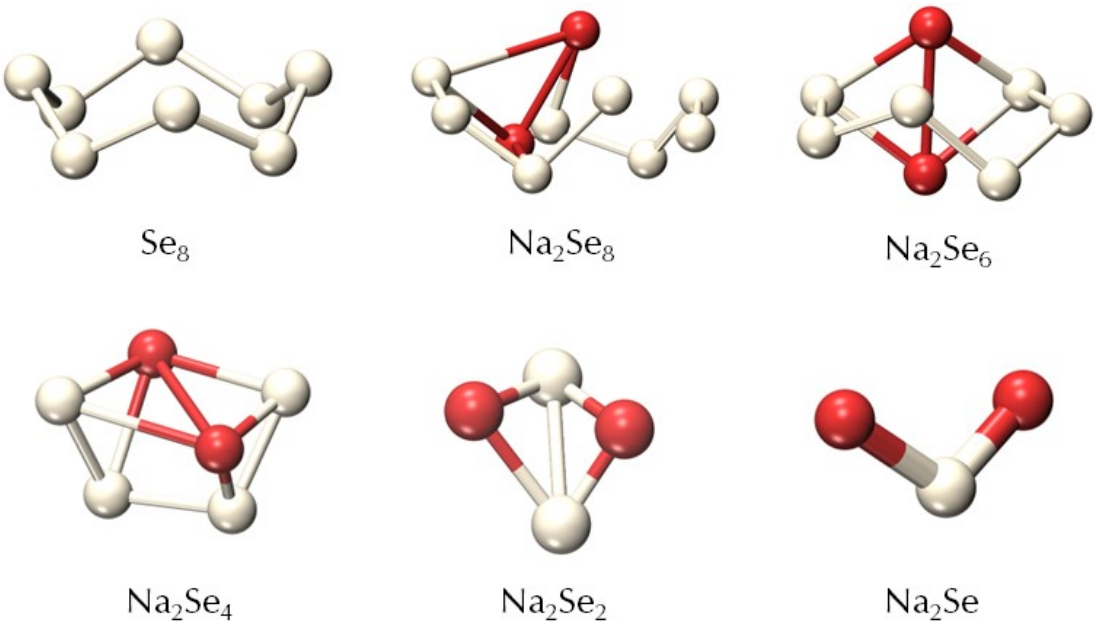


Fig. S7 Geometric optimization models of $Se_8$ rings and a series of $Na_2Se_x$.

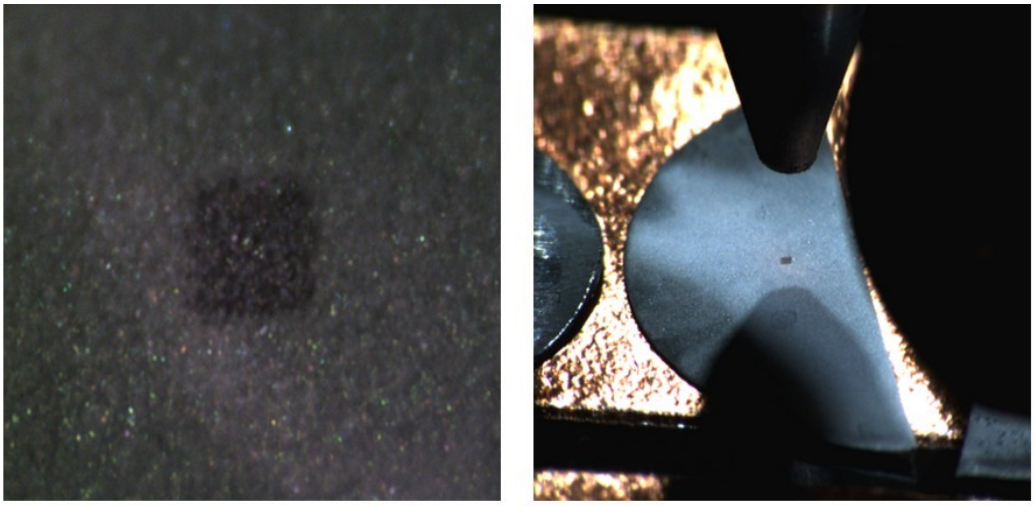


Fig. S8 Micro-optical photos of ToF-SIMS test of Na metal anode.

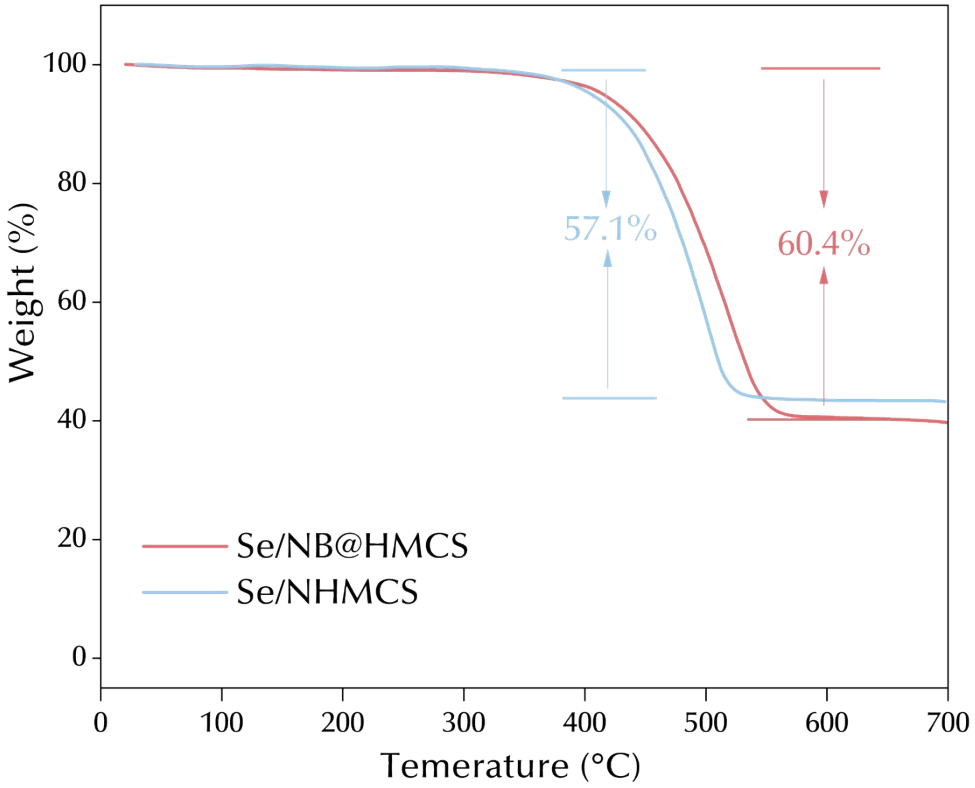


Fig. S9 Thermogravimetric analysis (TGA) curves of Se/NHMCS and Se/NB@HMCS in $N_2$ atmosphere.

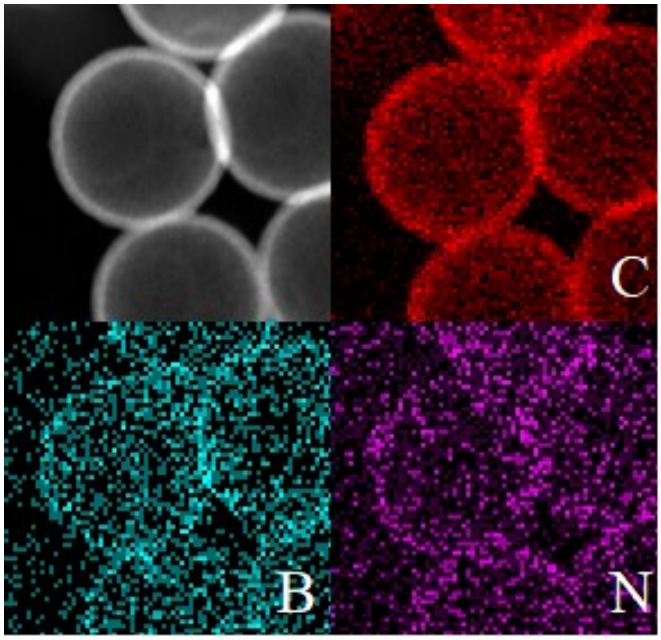


Fig. S10 EDX mapping images of NB@HMCS host.

**Table S1.** Surface elemental compositions of NB@HMCS determined by XPS.

| Element | Atomic percentage (at.%) |
|---|---|
| C | 86.8 |
| N | 5.5 |
| B | 3.4 |
| O | 4.3 |

**Table S2.** Relative percentages of different N species.

| N species | Relative percentage (%) |
|---|---|
| Pyrrolic N | 43.5 |
| Graphitic N | 28.4 |
| Pyridinic N | 18.6 |
| N-B | 9.5 |

**Table S3.** Relative percentages of different B species.

| B species | Relative percentage (%) |
|---|---|
| B-C | 51.8 |
| B-N | 34.6 |
| B-O | 13.6 |